AIAA JOURNAL
Vol. 34, No. 1, January 1996

# Shape Control of Vibrating Simply Supported Rectangular Plates

R. C. Batra* and X. Q. Liang†
*Virginia Polytechnic Institute and State University, Blacksburg, Virginia 24061-0219*
and
J. S. Yang‡
*Rensselaer Polytechnic Institute, Troy, New York 12180*

**We determine the optimum location of a given rectangular piezoceramic (PZT) actuator that will require the minimum voltage to annul the deflections of a simply supported rectangular linear elastic plate vibrating near one of its fundamental frequencies. Keeping the location of the centroid and the shape of the PZT fixed, we ascertain the voltage required as a function of the length of its diagonal to nullify the deflections of the plate.**

## Nomenclature

| | |
|---|---|
| $C_{\alpha\beta\gamma\delta}$ | = elasticities of a point |
| $D_{11}$, $D_{22}$ | = flexural rigidities of the plate |
| $E_{11}$, $E_{22}$, $E_{33}$ | = Young's moduli in 1, 2, and 3 directions |
| $e_{\gamma\delta}$ | = components of the infinitesimal strain tensor |
| $G_{12}$, $G_{31}$ | = shear moduli |
| $h^b$, $h^t$ | = thickness of actuators at the bottom and top surfaces |
| $u$ | = displacement of a point |
| $\ddot{u}$ | = acceleration of a point |
| $V$ | = applied voltage |
| $(x_1, x_2, x_3)$ | = coordinates of a point in a rectangular Cartesian coordinate system |
| $\nu_{12}$, $\nu_{13}$, $\nu_{23}$ | = Poisson's ratio |
| $\rho$ | = mass density |
| $\tau_{\alpha\beta}^{(i)}$ | = components of the Cauchy stress tensor at a point in the $i$th layer |

## Introduction

AN interesting problem in smart structures is to control the shape of a plate subjected to external disturbances. Here we consider the following problem. Assume that a simply supported rectangular plate with thin piezoelectric layers affixed to its bottom and top surfaces is vibrating freely at a frequency close to one of its natural frequencies. Find the optimum location and size of the piezoceramic (PZT) region on which a minimum voltage is applied to suppress the motion of the plate. We use the linear theory of elasticity to analyze this problem for the first few modes of vibration of the plate. We first envisage that the voltage is to be applied to a square area of fixed sides and investigate the location of its centroid that will require the minimum voltage to diminish the deflection of all points of the plate to essentially zero. Subsequently we locate the centroid of the rectangular PZT at the centroid of the square PZT found earlier and determine the length of its diagonal with the ratio of its sides always equal to that of the plate that will minimize the voltage. Even though we have not verified it, the conjecture is that if proper voltage at the appropriate frequencies is applied to several areas simultaneously, then the deflections of points of the plate can be reduced to essentially zero under a more general loading. For a plate vibrating in first two modes and the PZT excited with the frequency of the first mode, we found that only the first mode was canceled and there was no spill over to the second mode in the sense that its amplitude of vibration remained unchanged. Also, the results presented herein should help others formulate the problem more rigorously by using an optimization theory.

We note that piezoelectric elements have been extensively used to control the vibrations of a beam, e.g., see Baz and Poh,[1] Tzou and Tseng,[2] and Crawley and de Luis.[3] However, their use to control the shape and vibration of a thin plate has received less attention. Elastic plates with PZT films attached to their surfaces have been analyzed by using approximate two-dimensional plate theories. Three-dimensional equations of elasticity and the method of Fourier series have also been used to study deformations of elastic plates.[4–8] Here we use it to analyze dynamic deformations of a steadily vibrating orthotropic laminated plate with PZT layers bonded to its top and bottom surfaces. The goal is to determine the size of the PZT surface and the voltage to be applied to it so as to annul the deflections of all points of the plate.

## Formulation of the Problem

We use a fixed set of rectangular Cartesian coordinates to describe infinitesimal deformations of a laminated rectangular elastic plate with thin PZT layers affixed to its top and bottom surfaces, as shown in Fig. 1. Each laminate may be made of an orthotropic material and occupies the domain $0 \le x_1 \le a$, $0 \le x_2 \le b$ in the $x_1$–$x_2$ plane; however, in the $x_3$ direction points in the $i$th laminate satisfy $h^{(i-1)} \le x_3 \le h^{(i)}$. Thus the positions of the bottom and top surfaces as well as of the $(N-1)$ interfaces are given by $x_3 = 0, h^{(1)}, h^{(2)}, \ldots, h^{(N-1)}, h^{(N)} = h$. We use a superscript $i$ in parentheses to indicate quantities

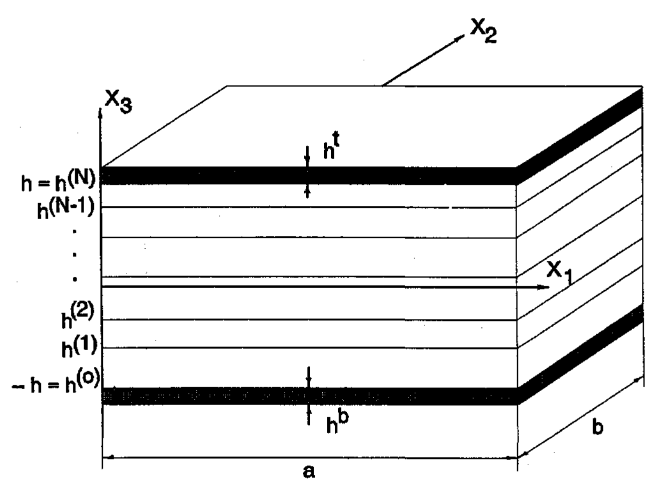


**Fig. 1 Schematic sketch of the problem studied.**

Received March 22, 1995; revision received July 8, 1995; accepted for publication July 10, 1995. 

*Clifton C. Garvin Professor, Department of Engineering Science and Mechanics.
†Graduate Student, Department of Engineering Science and Mechanics.
‡Postdoctoral Fellow, Department of Mechanical Engineering, Aeronautical Engineering and Mechanics.

for the $i$th layer. Equations governing the deformations of a material point of the $i$th layer are

$$\tau^{(i)}_{\alpha\beta,\beta} = \rho^{(i)}\ddot{u}^{(i)}_{\alpha}, \qquad \alpha, \beta = 1, 2, 3 \tag{1}$$

where a comma followed by an index $\beta$ implies partial differentiation with respect to $x_\beta$, a repeated index implies summation over the range of the index, and a superimposed dot implies the material time derivative that for infinitesimal deformations reduces to the partial time derivative. The constitutive relation for a linear elastic orthotropic material may be written as

$$\tau_{\alpha\beta} = C_{\alpha\beta\gamma\delta}e_{\gamma\delta} \tag{2}$$

$$2e_{\alpha\beta} = u_{\alpha,\beta} + u_{\beta,\alpha} \tag{3}$$

where we have dropped the superscript $i$ in parentheses. For an isotropic material

$$C_{\alpha\beta\gamma\nu} = \lambda\delta_{\alpha\beta}\delta_{\gamma\nu} + \mu(\delta_{\alpha\gamma}\delta_{\beta\nu} + \delta_{\alpha\nu}\delta_{\beta\gamma}) \tag{4}$$

where $\lambda$ and $\mu$ are Lamé constants, and $\delta_{\alpha\beta}$ is the Kronecker delta. The boundary conditions at the edges are

$$\tau_{11} = 0, \quad u_3 = 0, \quad u_2 = 0 \quad \text{at} \quad x_1 = 0, a \tag{5a}$$

$$\tau_{22} = 0, \quad u_3 = 0, \quad u_1 = 0 \quad \text{at} \quad x_2 = 0, b \tag{5b}$$

These boundary conditions simulate a simply supported plate characterized by the vanishing of the deflection and bending moment at the edges and have been previously employed for simply supported plates.[6–8] At the interface $x_3 = h^{(i)}$ between the $i$th and the $(i+1)$th layers, we have for $i = 1, 2, \ldots, N-1$,

$$\tau^{(i)}_{3\alpha} = \tau^{(i+1)}_{3\alpha}, \qquad u^{(i)}_{\alpha} = u^{(i+1)}_{\alpha} \quad \text{at} \quad x_3 = h^{(i)} \tag{6}$$

These imply the continuity of surface tractions and surface displacements at the interface, sometimes also referred to as the coherence conditions. Substitution from Eqs. (2) and (3) into Eqs. (1), (5), and (6) yields the governing equations, boundary conditions, and the coherence conditions in terms of displacements.

We model the piezoelectric actuators as thin piezoelectric films and use superscripts $b$ and $t$ to denote quantities for the bottom and top actuators, respectively. For the bottom actuator of thickness $h^b$ poled in the $x_3$ direction, the pertinent equations are

$$h^b\left(\tau^b_{11,1} + \tau^b_{21,2}\right) + \tau^{(1)}_{31}\big|_{x_3=-h} = \rho^b h^b \ddot{u}^b_1 \tag{7a}$$

$$h^b\left(\tau^b_{12,1} + \tau^b_{22,2}\right) + \tau^{(1)}_{32}\big|_{x_3=-h} = \rho^b h^b \ddot{u}^b_2 \tag{7b}$$

$$\tau^b_{11} = \bar{c}^b_{11}u^b_{1,1} + \bar{c}^b_{12}u^b_{2,2} - \bar{e}^b_{31}V^b(x_1, x_2, t)/h^b \tag{7c}$$

$$\tau^b_{22} = \bar{c}^b_{12}u^b_{1,1} + \bar{c}^b_{11}u^b_{2,2} - \bar{e}^b_{31}V^b(x_1, x_2, t)/h^b \tag{7d}$$

$$\tau^b_{12} = c^b_{66}\left(u^b_{1,2} + u^b_{2,1}\right) \tag{7e}$$

$$\tau^b_{11} = 0, \qquad u^b_2 = 0 \quad \text{at} \quad x_1 = 0, a \tag{7f}$$

$$\tau^b_{22} = 0, \qquad u^b_1 = 0 \quad \text{at} \quad x_2 = 0, b \tag{7g}$$

$$\begin{aligned} &\tau^{(1)}_{33} = \rho^b h^b \ddot{u}^{(1)}_3, \qquad u^{(1)}_1 = u^b_1, \quad \text{and} \\ &u^{(1)}_2 = u^b_2 \quad \text{at} \quad x_3 = -h \end{aligned} \tag{7h}$$

Equations (7a) and (7b) express the balance of linear momentum obtained after integrating through the thickness and assuming that displacements of the PZT layer are independent of $x_3$. The constitutive relations of the PZT are given by Eqs. (7c–7e) with $V^b$ being the voltage difference across its surfaces, and boundary conditions (7f) and (7g) are equivalent to the vanishing of moments and displacements at the edges. The coherency or continuity conditions at the interface $x_3 = -h$ are given by Eq. (7h).

We note that equations analogous to Eqs. (7) give deformations of the top PZT layer and are omitted.

## Time Harmonic Vibrations

### Reduction of Governing Equations

We assume that the plate is vibrating harmonically at a frequency close to one of its natural frequencies with no voltage applied to the PZTs. Let the corresponding displacement field be given by $\tilde{u}^0_\alpha(x_1, x_2, x_3)$. The objective is to find the optimum size and location of the rectangular area on the top and bottom PZT layers where a harmonically varying voltage with frequency equal to that of the plate and the least amplitude should be applied so as to annul the deflections of all points of the plate. Since we are analyzing a linear problem, the resulting displacement of a point equals the sum of the initial displacement and that induced by the applied voltage. Next we attempt to find the latter.

Let the time harmonic driving voltage be given by

$$V^b(x_1, x_2, t) = \bar{V}^b(x_1, x_2)e^{i\omega t} \tag{8a}$$

$$V^t(x_1, x_2, t) = \bar{V}^t(x_1, x_2)e^{i\omega t} \tag{8b}$$

For steady-state vibrations all field quantities have the same time dependence,

$$u^{(i)}_\alpha(x_1, x_2, x_3, t) = \tilde{u}^{(i)}_\alpha(x_1, x_3, x_3)e^{i\omega t}, \qquad \alpha = 1, 2, 3 \tag{9a}$$

$$u^t_\alpha(x_1, x_2, t) = \tilde{u}^t_\alpha(x_1, x_2)e^{i\omega t}, \qquad \alpha = 1, 2 \tag{9b}$$

$$u^b_\alpha(x_1, x_2, t) = \tilde{u}^b_\alpha(x_1, x_2)e^{i\omega t}, \qquad \alpha = 1, 2 \tag{9c}$$

Substitution of Eqs. (9) and constitutive relations (2) and (7c–7e) into Eqs. (1), (6), (7a), (7b), and (7f–7h) yields following equations for the determination of $\tilde{u}^{(i)}_\alpha$, $\tilde{u}^t_\alpha$, and $\tilde{u}^b_\alpha$, where we have dropped the superimposed tildes on $u^{(i)}_\alpha$, $u^t_\alpha$, and $u^b_\alpha$:

$$\begin{aligned} &c^{(i)}_{11}u^{(i)}_{1,11} + c^{(i)}_{66}u^{(i)}_{1,22} + c^{(i)}_{55}u^{(i)}_{1,33} + \left[c^{(i)}_{12} + c^{(i)}_{66}\right]u^{(i)}_{2,12} \\ &\quad + \left[c^{(i)}_{13} + c^{(i)}_{55}\right]u^{(i)}_{3,13} = -\rho^{(i)}\omega^2 u^{(i)}_1 \\ &\left[c^{(i)}_{12} + c^{(i)}_{66}\right]u^{(i)}_{1,12} + c^{(i)}_{66}u^{(i)}_{2,11} + c^{(i)}_{22}u^{(i)}_{2,22} + c^{(i)}_{44}u^{(i)}_{2,33} \\ &\quad + \left[c^{(i)}_{23} + c^{(i)}_{44}\right]u^{(i)}_{3,23} = -\rho^{(i)}\omega^2 u^{(i)}_2 \\ &\left[c^{(i)}_{13} + c^{(i)}_{55}\right]u^{(i)}_{1,13} + \left[c^{(i)}_{23} + c^{(i)}_{44}\right]u^{(i)}_{2,23} + c^{(i)}_{55}u^{(i)}_{3,11} \\ &\quad + c^{(i)}_{44}u^{(i)}_{3,22} + c^{(i)}_{33}u^{(i)}_{3,33} = -\rho^{(i)}\omega^2 u^{(i)}_3 \end{aligned} \tag{10a}$$

$$\begin{aligned} &c^{(i)}_{11}u^{(i)}_{1,1} + c^{(i)}_{12}u^{(i)}_{2,2} + c^{(i)}_{13}u^{(i)}_{3,3} = 0, \qquad u^{(i)}_3 = 0 \\ &u^{(i)}_2 = 0 \quad \text{at} \quad x_1 = 0, a \\ &c^{(i)}_{12}u^{(i)}_{1,1} + c^{(i)}_{22}u^{(i)}_{2,2} + c^{(i)}_{23}u^{(i)}_{3,3} = 0, \qquad u^{(i)}_3 = 0 \\ &u^{(i)}_1 = 0 \quad \text{at} \quad x_2 = 0, b \\ &c^{(i)}_{55}\left[u^{(i)}_{3,1} + u^{(i)}_{1,3}\right] = c^{(i+1)}_{55}\left[u^{(i+1)}_{3,1} + u^{(i+1)}_{1,3}\right] \quad \text{at} \quad x_3 = h^{(i)} \\ &c^{(i)}_{44}\left[u^{(i)}_{2,3} + u^{(i)}_{3,2}\right] = c^{(i+1)}_{44}\left[u^{(i+1)}_{2,3} + u^{(i+1)}_{3,2}\right] \quad \text{at} \quad x_3 = h^{(i)} \\ &c^{(i)}_{13}u^{(i)}_{1,1} + c^{(i)}_{23}u^{(i)}_{2,2} + c^{(i)}_{33}u^{(i)}_{3,3} = c^{(i+1)}_{13}u^{(i+1)}_{1,1} \\ &\quad + c^{(i+1)}_{23}u^{(i+1)}_{2,2} + c^{(i+1)}_{33}u^{(i+1)}_{3,3} \quad \text{at} \quad x_3 = h^{(i)} \\ &u^{(i)}_1 = u^{(i+1)}_1, \qquad u^{(i)}_2 = u^{(i+1)}_2 \\ &u^{(i)}_3 = u^{(i+1)}_3 \quad \text{at} \quad x_3 = h^{(i)} \end{aligned} \tag{10b}$$

$$\begin{aligned} &h^b\bar{c}^b_{11}u^b_{1,11} + h^b c^b_{66}u^b_{1,22} + h^b\left(\bar{c}^b_{12} + c^b_{66}\right)u^b_{2,12} \\ &\quad + c^{(1)}_{55}\left[u^{(1)}_{3,1} + u^{(1)}_{1,3}\right]\big|_{x_3=-h} = -\rho^b h^b\omega^2 u^b_1 \\ &h^b\left(\bar{c}^b_{12} + c^b_{66}\right)u^b_{1,12} + h^b c^b_{66}u^b_{2,11} + h^b\bar{c}^b_{11}u^b_{2,22} \\ &\quad + c^{(1)}_{44}\left[u^{(1)}_{3,2} + u^{(1)}_{2,3}\right]\big|_{x_3=-h} = -\rho^b h^b\omega^2 u^b_2 \\ &h^b\bar{c}^b_{11}u^b_{1,1} = \bar{e}^b_{31}\bar{V}^b, \qquad u^b_2 = 0 \quad \text{at} \quad x_1 = 0, a \\ &h^b\bar{c}^b_{11}u^b_{2,2} = \bar{e}^b_{31}\bar{V}^b, \qquad u^b_1 = 0 \quad \text{at} \quad x_2 = 0, b \end{aligned} \tag{10c}$$

$$
\begin{aligned}
&h^t\bar{c}^t_{11}u^t_{1,11} + h^t c^t_{66}u^t_{1,22} + h^t\left(\bar{c}^t_{12} + c^t_{66}\right)u^t_{2,12} \\
&\quad - c^{(N)}_{55}\left[u^{(N)}_{3,1} + u^{(N)}_{1,3}\right]\Big|_{x_3=h} = -\rho^t h^t\omega^2 u^t_1 \\
&h^t\left(\bar{c}^t_{12} + c^t_{66}\right)u^t_{1,12} + h^t c^t_{66}u^t_{2,11} + h^t\bar{c}^t_{11}u^t_{2,22} \\
&\quad - c^{(N)}_{44}\left[u^{(N)}_{3,2} + u^{(N)}_{2,3}\right]\Big|_{x_3=h} = -\rho^t h^t\omega^2 u^t_2 \\
&h^t\bar{c}^t_{11}u^t_{1,1} = \bar{e}^t_{31}\bar{V}^t, \qquad u^t_2 = 0 \quad \text{at} \quad x_1 = 0, a \\
&h^t\bar{c}^t_{11}u^t_{2,2} = \bar{e}^t_{31}\bar{V}^t, \qquad u^t_1 = 0 \quad \text{at} \quad x_2 = 0, b
\end{aligned} \tag{10d}
$$

$$
\begin{aligned}
&c^{(1)}_{13}u^{(1)}_{1,1} + c^{(1)}_{23}u^{(1)}_{2,2} + c^{(1)}_{33}u^{(1)}_{3,3} = -\rho^b h^b\omega^2 u^{(1)}_3 \\
&u^{(1)}_1 = u^b_1, \qquad u^{(1)}_2 = u^b_2 \quad \text{at} \quad x_3 = -h \\
&-\left[c^{(N)}_{13}u^{(N)}_{1,1} + c^{(N)}_{23}u^{(N)}_{2,2}c^{(N)}_{33}u^{(N)}_{3,3}\right] = -\rho^t h^t\omega^2 u^{(N)}_3 \\
&u^{(N)}_1 = u^t_1, \qquad u^{(N)}_2 = u^t_2 \quad \text{at} \quad x_3 = h
\end{aligned} \tag{10e}
$$

**Solutions for the Laminates**

The solution procedure is similar to that detailed in Ref. 8 and is therefore briefly described herein. To solve Eqs. (10) we assume that

$$
\begin{aligned}
u_1(x_1, x_2, x_3, t) &= \sum_{m,n=1}^{\infty} a_{1mn}(x_3)\cos\alpha_m x_1 \sin\beta_n x_2 \\
u_2(x_1, x_2, x_3, t) &= \sum_{m,n=1}^{\infty} a_{2mn}(x_3)\sin\alpha_m x_1 \cos\beta_n x_2 \\
u_3(x_1, x_2, x_3, t) &= \sum_{m,n=1}^{\infty} a_{3mn}(x_3)\sin\alpha_m x_1 \sin\beta_n x_2 \\
\alpha_m = m\pi/a, &\qquad \beta_n = n\pi/b
\end{aligned} \tag{11}
$$

which satisfy all boundary conditions at the edges $x_1 = 0, a$ and $x_2 = 0, b$. Substitution of Eqs. (11) into the governing Eqs. (10) yields the following ordinary differential equations for $a_{\alpha mn}(x_3)$:

$$
\begin{aligned}
&-c^{(i)}_{11}\alpha^2_m a^{(i)}_{mn} - c^{(i)}_{66}\beta^2_n a^{(i)}_{mn} + c^{(i)}_{55}a^{(i)}_{mn,33} - \left[c^{(i)}_{12} + c^{(i)}_{66}\right]\alpha_m\beta_n b^{(i)}_{mn} \\
&\quad + \left[c^{(i)}_{13} + c^{(i)}_{55}\right]\alpha_m c^{(i)}_{mn,3} = -\rho^{(i)}\omega^2 a^{(i)}_{mn} \\
&-\left[c^{(i)}_{12} + c^{(i)}_{66}\right]\alpha_m\beta_n a^{(i)}_{mn} - c^{(i)}_{66}\alpha^2_m b^{(i)}_{mn} - c^{(i)}_{22}\beta^2_n b^{(i)}_{mn} + c^{(i)}_{44}b^{(i)}_{mn,33} \\
&\quad + \left[c^{(i)}_{23} + c^{(i)}_{44}\right]\beta_n c^{(i)}_{mn,3} = -\rho^{(i)}\omega^2 b^{(i)}_{mn} \\
&-\left[c^{(i)}_{13} + c^{(i)}_{55}\right]\alpha_m a^{(i)}_{mn,3} - \left[c^{(i)}_{23} + c^{(i)}_{44}\right]\beta_n b^{(i)}_{mn,3} - c^{(i)}_{55}\alpha^2_m c^{(i)}_{mn} \\
&\quad - c^{(i)}_{44}\beta^2_n c^{(i)}_{mn} + c^{(i)}_{33}c^{(i)}_{mn,33} = -\rho^{(i)}\omega^2 c^{(i)}_{mn}
\end{aligned} \tag{12}
$$

We now assume that (no sum on repeated indices)

$$
a_{\alpha mn}(x_3) = A_{\alpha mn}e^{\eta_{mn}x_3} \tag{13}
$$

where $A_{\alpha mn}$ are undetermined constants. Relation (13) when substituted into Eq. (12) yields a set of linear homogeneous equations for the determination of $A_{\alpha mn}$; the coefficients of these equations involve the elastic constants for the material of the laminate. The necessary and sufficient condition for these equations to have a nontrivial solution is the following cubic equation for $(\eta_{mn})^2$:

$$
(\eta_{mn})^6 + a(\eta_{mn})^4 + b(\eta_{mn})^2 + c = 0 \tag{14}
$$

Explicit expressions for $a$, $b$, and $c$ in terms of the elasticities of the laminate are given in Ref. 8. For a real root $\eta_{mnp}$ with $p = 1, 2, \ldots, 6$, of Eq. (14), we have, with no sum on $m$ and $n$, but summed on $p$,

$$
a_{\alpha mn}(x_3) = D_{mnp}F_{\alpha mnp}e^{\eta_{mnp}x_3} \tag{15}
$$

where $D_{mnp}$ is an arbitrary constant and $F_{\alpha mnp}$ is a function of $\eta_{mnp}$ and the material parameters. For a complex root $\eta_{mnp} = \xi_{mnp} + i\zeta_{mnp}$ of Eq. (14), one can show that Eq. (15) still holds with $F_{\alpha mnp}$ involving $\cos(\xi_{mnp}x_3)$ and $\sin(\zeta_{mnp}x_3)$ in addition to the material elasticities. We note that, for a few values of $\omega$, Eq. (14) may have repeated roots; it is more likely to occur for an isotropic material. We exclude those special values of $\omega$.

The continuity conditions at the interface $x_3 = h^{(i)}$ require that

$$
\left[D^{(i)}_{mnp}\right] = \left[T^{(i)}\right]\left[D^{(i+1)}_{mnp}\right] \tag{16}
$$

where $[D^{(i)}_{mnp}]$ is a $6 \times 1$ matrix (for $p = 1, 2, \ldots, 6$), and $[T^{(i)}]$ is a $6 \times 6$ matrix whose elements are functions of $F^{(i)}_{\alpha mnp}$ and $F^{(i+1)}_{\alpha mnp}$ evaluated at $x_3 = h^{(i)}$. Equation (16) is a recursive relation between constants for the $i$th and $(i + 1)$th laminate.

**Solutions for the Actuators**

We assume that

$$
\begin{aligned}
u^b_1(x_1, x_2) &= \sum_{m,n=1}^{\infty} D^b_{1mn}\cos\alpha_m x_1 \sin\beta_n x_2 \\
u^b_2(x_1, x_2) &= \sum_{m,n=1}^{\infty} D^b_{2mn}\sin\alpha_m x_1 \cos\beta_n x_2
\end{aligned} \tag{17}
$$

give the displacement field for the bottom actuator. To avoid term by term differentiation and to take care of the nonhomogeneous boundary conditions at the same time, we multiply equations obtained from Eq. (7a) by $\cos\alpha_m x_1 \sin\beta_n x_2$ and that obtained from Eq. (7b) by $\sin\alpha_m x_1 \cos\beta_n x_2$ and integrate the resulting equations over $0 < x_1 < a$ and $0 < x_2 < b$. With integration by parts and the use of boundary conditions (7f) and (7g), we arrive at the following:

$$
\begin{aligned}
&\sum_{p=1}^{6} R^{(1)}_{mnp}(-h)D^{(1)}_{mnp} + h^b\left(\rho^b\omega^2 - \bar{c}^b_{11}\alpha^2_m - c^b_{66}\beta^2_n\right)D^b_{1mn} \\
&\quad - h^b\left(\bar{c}^b_{12} + c^b_{66}\right)\alpha_m\beta_n D^b_{2mn} \\
&\quad = \frac{4\bar{e}^b_{31}}{ab}\alpha_m \int_0^a\int_0^b \bar{V}^b \sin\alpha_m x_1 \sin\beta_n x_2 \,\mathrm{d}x_1\,\mathrm{d}x_2
\end{aligned} \tag{18}
$$

$$
\begin{aligned}
&\sum_{p=1}^{6} Q^{(1)}_{mnp}(-h)D^{(1)}_{mnp} - h^b\left(\bar{c}^b_{12} + c^b_{66}\right)\alpha_m\beta_n D^b_{1mn} \\
&\quad + h^b\left(\rho^b\omega^2 - c^b_{66}\alpha^2_m - \bar{c}^b_{11}\beta^2_n\right)D^b_{2mn} \\
&\quad = \frac{4\bar{e}^b_{31}}{ab}\beta_n \int_0^a\int_0^b \bar{V}^b \sin\alpha_m x_1 \sin\beta_n x_2 \,\mathrm{d}x_1\,\mathrm{d}x_2
\end{aligned} \tag{19}
$$

where $R_{mnp}$ and $Q_{mnp}$ are linear functions of $F_{\alpha mnp}$ and $F_{\alpha mnp,3}$, and $\bar{V}^b$ is a function of $x_1$ and $x_2$. The continuity conditions (7h) at the interface between the plate and the bottom actuator give additional conditions on $D_{mnp}$, $D^b_{1mn}$, and $D^b_{2mn}$; similar equations can be obtained for the top actuator. The end result is that we get a set of 16 algebraic equations for the 16 unknowns $D^{(1)}_{mnp}$, $D^{(N)}_{mnp}$, $D^b_{1mn}$, $D^b_{2mn}$, $D^t_{1mn}$, and $D^t_{2mn}$. Knowing $\omega$ and $\bar{V}$, we can solve for these 16 unknowns and hence for displacements and stresses at any point of the structure.

## Numerical Results

To elucidate that the deflections of a vibrating plate can be controlled by applying suitable voltage to a part of the top and bottom PZT layers, we consider a graphite/epoxy plate with PZT-G1195 actuators affixed to its top and bottom surfaces. The material parameters for the graphite/epoxy are

$$
\begin{aligned}
E_{11} &= 150\,\text{GPA}, & E_{22} &= E_{33} = 9\,\text{GPa} \\
\nu_{12} &= \nu_{23} = \nu_{13} = 0.3, & G_{12} &= G_{31} = 7.1\,\text{GPa} \\
G_{23} &= 2.5\,\text{GPa}, & \rho &= 1600\,\text{kg/m}^3
\end{aligned} \tag{20}
$$

and those for the PZT are

$$e^b = e^t = \begin{bmatrix} 0 & 0 & -2.1 \\ 0 & 0 & -2.1 \\ 0 & 0 & 9.5 \\ 0 & 9.2 & 0 \\ 9.2 & 0 & 0 \\ 0 & 0 & 0 \end{bmatrix}^T \frac{C}{m^2}$$

$$c^b = c^t = \begin{bmatrix} 148 & 76.2 & 74.2 & 0 & 0 & 0 \\ & 148 & 74.2 & 0 & 0 & 0 \\ & & 131 & 0 & 0 & 0 \\ & \text{Symmetric} & & 25.4 & 0 & 0 \\ & & & & 25.4 & 0 \\ & & & & & 35.9 \end{bmatrix} \text{GPa} \quad (21)$$

$$\rho^b = \rho^t = 7500\,\text{kg/m}^3$$

For geometric dimensions, we choose $a = 40$ cm, $b = 30$ cm, $h = 1$ mm, and $h^b = h^t = 0.1$ mm. Even though the preceding analysis is valid for a laminated elastic plate, results presented herein are for one lamina. We apply a uniform voltage to a rectangular region of the PZT surface and zero voltage to the rest of the PZT surface.

The structure has a series of natural bending vibration frequencies that can be ordered as $\omega_{mn}, m, n = 1, 2, 3, \ldots$. The free bending vibration modes corresponding to $\omega_{11}, \omega_{31}, \omega_{13}, \omega_{33} \ldots$, are symmetric about both $x_1 = a/2$ and $x_2 = b/2$, and those corresponding to $\omega_{12}, \omega_{21}, \omega_{22}, \ldots$, are antisymmetric about either $x_1 = a/2$ or $x_2 = b/2$, or both. The natural frequencies of the structure can be roughly estimated from the results of the plate theory. When the inertia and rigidity of the actuators are neglected, we have

$$\omega_{mn} \approx \frac{\pi^2}{\sqrt{2h\rho}} \left[ D_{11}\left(\frac{m}{a}\right)^4 + 2(D_{12} + 2D_{66}) \times \left(\frac{m}{a}\right)^2 \left(\frac{n}{b}\right)^2 + D_{22}\left(\frac{n}{b}\right)^4 \right]^{\frac{1}{2}} \quad (22)$$

or

$$\Omega_{mn} = \omega_{mn} \bigg/ \left[ \frac{\pi^2}{a^2}\left(\frac{D_{11}}{\rho 2h}\right)^{\frac{1}{2}} \right] \approx \left[ m^4 + 2\frac{(D_{12} + 2D_{66})}{D_{11}} m^2 \left(\frac{a}{b}n\right)^2 + \frac{D_{22}}{D_{11}}\left(\frac{a}{b}n\right)^4 \right]^{\frac{1}{2}} \quad (23)$$

where $\Omega_{mn}$ is the normalized natural frequency. Values of $\Omega_{mn}$ computed from Eq. (23) are compared in Table 1 with those obtained from the present method for the two cases when the PZTs are considered and when their effect is made negligible by assigning very small values to their thicknesses and the mass density. Values of $\Omega_{mn}$ by the present method are obtained by plotting $|U_3(a/2, b/2, 0)| = |u_3(a/2, b/2, 0)| hc_{31}^b h^b / a^2 e_{31}^b V^b$, the normalized deflection of the centroid of the plate, as a function of the normalized forcing frequency $\Omega = \omega / [(\pi^2/a^2)(D_{11}/\rho 2h)^{1/2}]$ in Fig. 2. It is seen that $U_3(a/2, b/2, 0)$ becomes large at certain discrete values of $\Omega$, which signifies the resonance phenomenon. Those values of $\Omega$ at which resonances occur should be in the sequence of $\Omega_{11}, \Omega_{12}, \Omega_{21}, \Omega_{13}, \Omega_{22}, \Omega_{23}, \Omega_{31}, \Omega_{32}, \Omega_{33}, \ldots$. It is evident from the values listed in the table that the currently computed values of $\Omega_{mn}$ are close to those obtained from the plate theory; it is to be expected since the plate theory gives good results for low-frequency vibrations. However, the present method will compute high frequencies accurately too. Also, the frequencies are shifted noticeably when thin layers of PZTs are affixed to the top and bottom surfaces of the plate.

When $\Omega$ is near $\Omega_{11}, \Omega_{12}, \Omega_{13}$, etc., at most 20 terms are needed for $u_3(a/2, b/2, 0)$ to be computed accurately to four significant digits. For higher values of $\Omega$, higher order modes also become important, and therefore more terms are needed in the series. For results presented herein, 800 terms in the Fourier series are summed to ensure sufficient accuracy.

**Table 1 Values of resonant frequencies $\Omega_{mn}$ for the graphite/epoxy plate as computed by the plate theory and the present method and also by the present method for the plate with PZTs bonded to the top and bottom surfaces[a]**

| $n$ \ $m$ | 1 | 2 | 3 | Case |
|---|---|---|---|---|
| 1 | 1.260 | 4.217 | 9.208 | 1 |
| | 1.260 | 4.170 | 9.170 | 2 |
| | 1.455 | 4.065 | 8.550 | 3 |
| 2 | 2.373 | 5.041 | 9.919 | 1 |
| | 2.330 | 5.040 | 9.880 | 2 |
| | 3.585 | 5.790 | 10.035 | 3 |
| 3 | 4.466 | 6.761 | 11.343 | 1 |
| | 4.460 | 6.710 | 11.290 | 2 |
| | 7.350 | 9.225 | 13.005 | 3 |

[a]Case 1, plate theory; case 2, present method, plate without PZTs; case 3, present method, plate with PZTs.

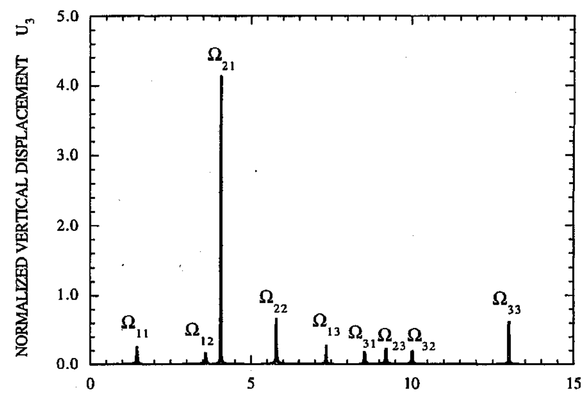


**Fig. 2 Normalized deflection of the centroid, $|U_3(a/2, b/2, 0)| = |u_3(a/2, b/2, 0)| hc_{31}^b h^b / a^2 e_{31}^b V$, as a function of the nondimensional forcing frequency $\Omega = \omega / [(\pi^2/a^2)(D_{11}/\rho 2h)^{1/2}]$; natural frequencies of the structure.**

We now assume that the structure is vibrating at a frequency close to one of its natural frequencies with the displacement field given by

$$u_3^0 = 0.3 \sin(m\pi x_1/a) \sin(n\pi x_2/b) e^{i\Omega_{mn}t} \; mm$$
$$u_1^0 = u_2^0 = 0 \quad (24)$$

We apply a voltage $\pm V_0 e^{i\Omega_{mn}t}$ to a square region of the top and bottom PZTs with zero voltage applied to the rest of the PZT surfaces. The reason for selecting a square region is to evaluate exactly the integrals in Eqs. (18) and (19). We first keep the size of the square region to which nonzero voltage is applied fixed and for a given location $(\bar{x}_1, \bar{x}_2)$ of its centroid, find the voltage to be applied to the square region that will reduce the magnitude of vertical deflections of all points of the plate to less than one-hundredth of the amplitude of their initial vibrations. Then with the centroid of the region located at the point that requires the least voltage in the preceding exercise, we vary the length of the sides of the rectangular region, but keep the ratio of their lengths as $a/b$, and find the applied voltage that will effectively annul the deflections of all points of the plate.

Figures 3a–3d depict the voltage required to annul the deflections of the plate as a function of the coordinates of the centroid of the $6 \times 6$ cm region for modes 11, 13, 21, and 22, respectively; the normalized frequencies of the applied voltage and the structure equal 1.46, 7.35, 4.06, and 5.79, respectively. It is clear that the needed voltage is minimum (maximum) when the centroid of the square region is located at points where $|u_3^0|$ assumes maximum (zero) values. Thus the most effective location of the square PZT region is points where the amplitude of initial vibrations of

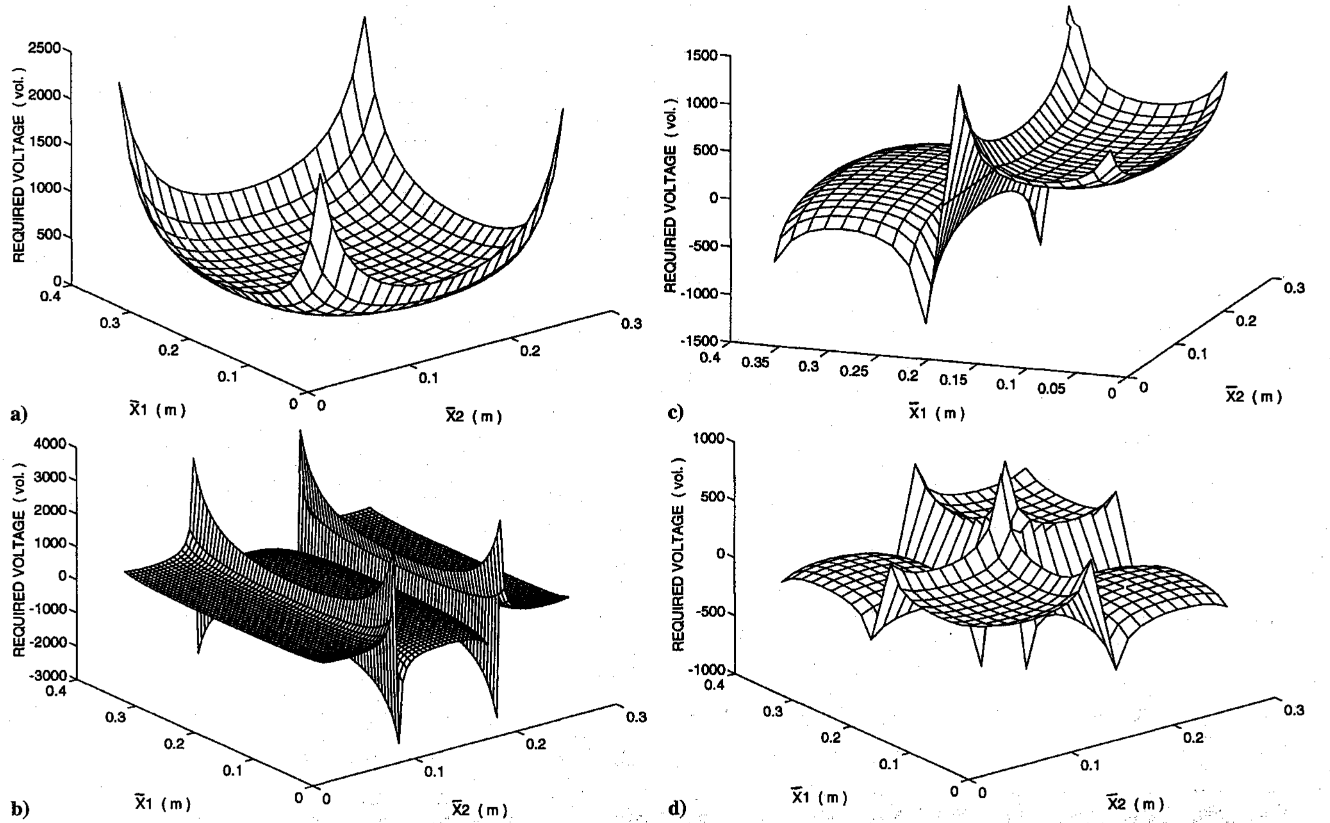


**Fig. 3 Voltage required to suppress the deflections of points on the plate diagonal as a function of the location of the centroid of the 6 × 6 cm PZT region that is excited. The plate is vibrating steadily at a frequency close to a) $\Omega_{11}$, b) $\Omega_{13}$, c) $\Omega_{21}$, and d) $\Omega_{22}$.**

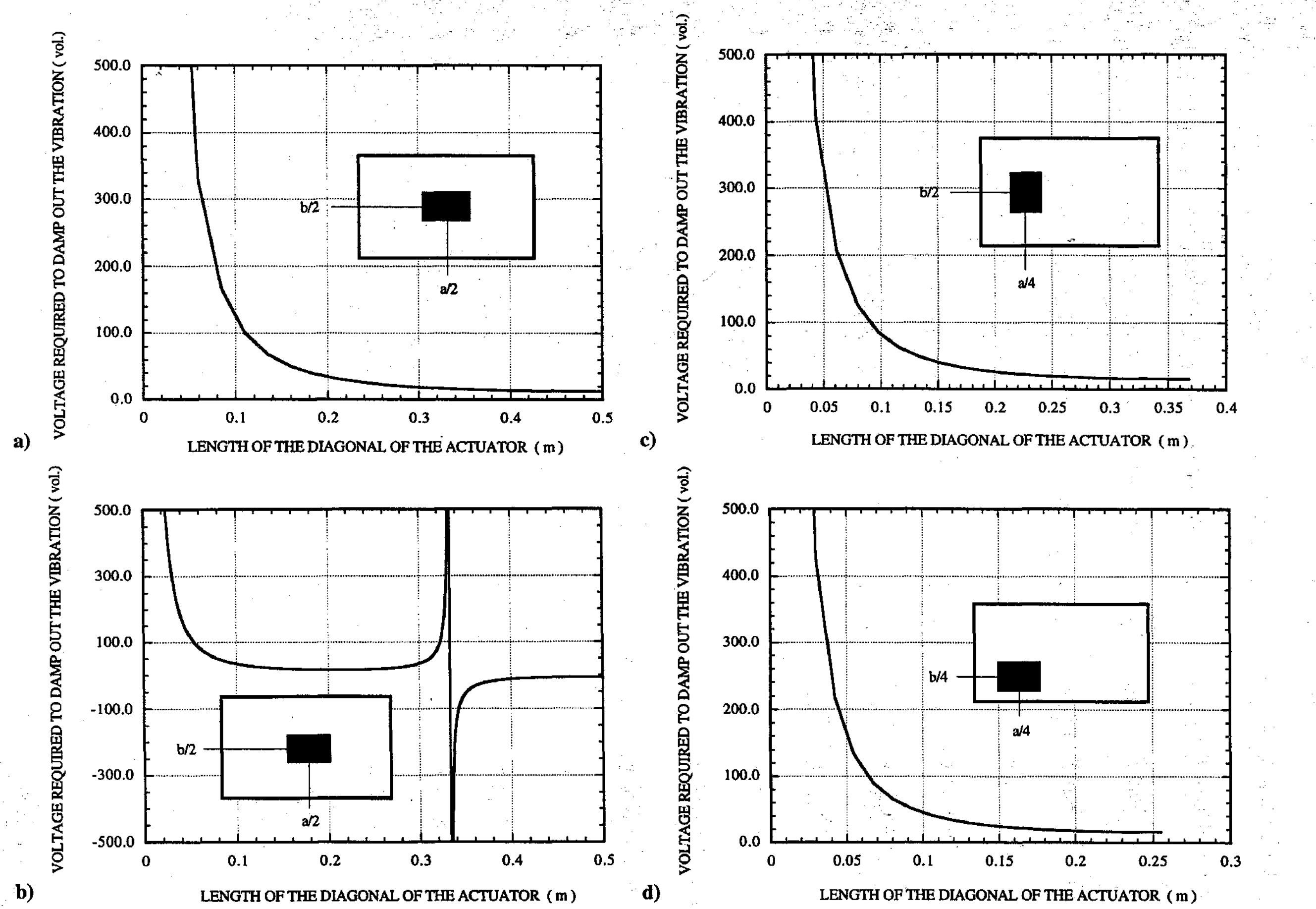


**Fig. 4 Voltage required to suppress the deflections of points on the plate diagonal as a function of the length of the diagonal of the rectangular excited PZT region with its centroid located at an optimum location. The plate is steadily vibrating at a frequency close to a) $\Omega_{11}$, b) $\Omega_{13}$, c) $\Omega_{21}$, and d) $\Omega_{22}$.**

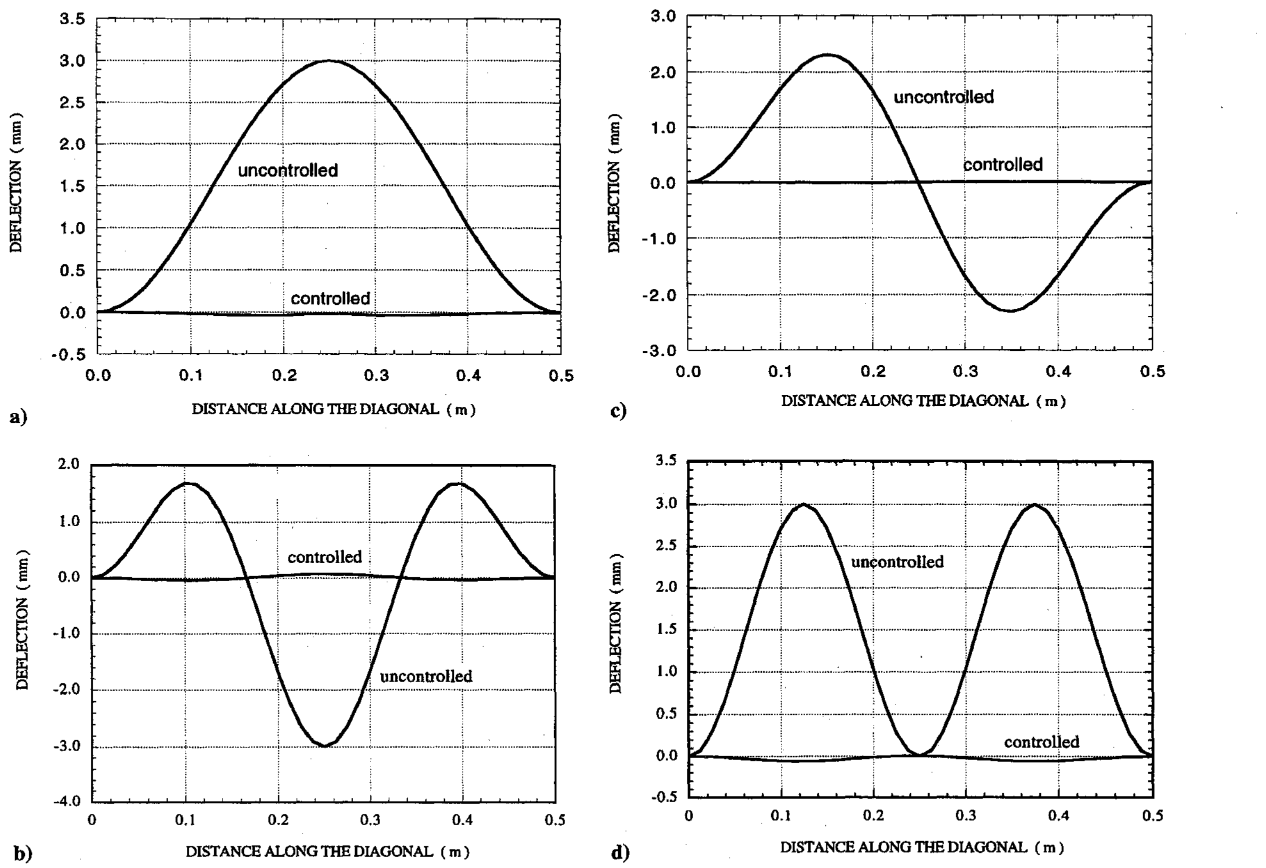


**Fig. 5 Controlled and uncontrolled deformed shape of a diagonal of the plate when it is vibrating steadily at a frequency close to a) $\Omega_{11}$, b) $\Omega_{13}$, c) $\Omega_{21}$, and d) $\Omega_{22}$.**

the plate is maximum. Whereas for mode 11, there is one optimum location, i.e., $(a/2, b/2)$ of the centroid of the excited square PZT region; for mode 13 there are three equally good locations, viz., $(a/2, b/2)$, $(a/2, b/6)$, and $(a/2, 5b/6)$; for mode 12 equally effective locations are $(a/4, b/2)$ and $(3a/4, b/2)$; and for mode 22 the four locations that require minimum value of $V_0$ are $(a/4, b/4)$, $(a/4, 3b/4)$, $(3a/4, b/4)$, and $(3a/4, 3b/4)$. We note that the sign of the voltage of the top and bottom PZT layers may have to be switched if all of the excited region crosses a nodal line. Figures 4a–4d depict the variation of the voltage required as a function of the length of the diagonal of the rectangular region on which a voltage is applied. These plots illustrate that the voltage required to suppress the deflections of points of the plate decreases rapidly as the size of the excited region is increased provided that this region is away from the nodal lines. However, when the excited region approaches nodal lines, the voltage required to suppress the vibrations decreases rather slowly. The magnitude of the slope of these curves gradually approaches zero so that a point of diminishing return is reached when the boundaries of the excited region touch but do not cross the nodal lines. For mode 13, the required voltage suddenly increases when the excited PZT region extends over plate particles vibrating in opposite directions or crosses over the nodal line. Figures 5a–5d depict the deflected shape of the diagonal of the plate both when similarly situated optimum rectangular regions of the top and bottom PZT layers with centroids at the optimum location are and are not activated; the voltage applied equals 159.8, 44.8, 103.4, and $57.6V$, respectively, for modes 11, 13, 21, and 22. It is clear that the deflections of points of a diagonal of the plate for each one of the four modes considered have been annulled.

We have plotted in Fig. 6 the distribution of the nondimensional shear stress, $T_{31}(x_1, x_2, h) = \tau_{31}(x_1, x_2, h)h^b/e_{31}^b\bar{V}^b$, at the interface between the plate and the top PZT for the structure vibrating at a normalized frequency of 1.46, which is close to $\Omega_{11}$. It is clear that the shear stress is high at the edges of the excited square region; for

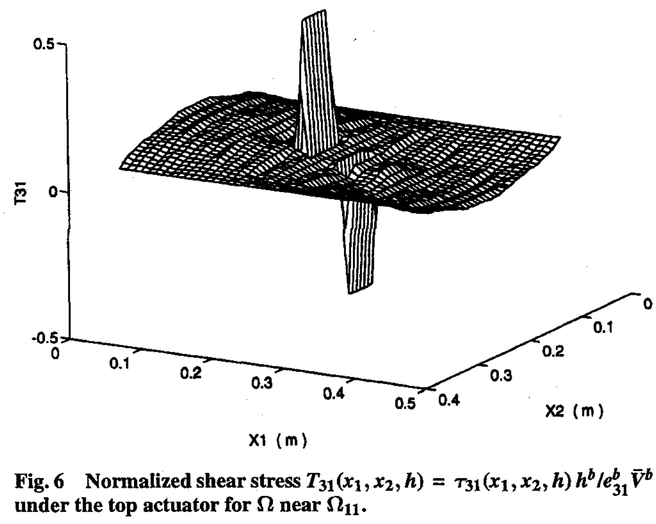


**Fig. 6 Normalized shear stress $T_{31}(x_1, x_2, h) = \tau_{31}(x_1, x_2, h)\,h^b/e_{31}^b\bar{V}^b$ under the top actuator for $\Omega$ near $\Omega_{11}$.**

other modes of vibration, the shear stress is found to be high either at the other two edges of the excited square region and/or at the four corners. The high value of the shear stress at a point may result in delamination of the PZT layer there. The high value of the shear stress at a corner may be eliminated or reduced considerably by exciting a circular region of the PZT layer, but it could not be verified because of the difficulty in evaluating exactly the integrals in Eqs. (18) and (14). The numerical evaluation of these integrals results in high values of $T_{31}$ at the quadrature points used to evaluate these integrals.

Computed values of stress components $T_{11}$, $T_{22}$, and $T_{12}$ within the top PZT indicated that $T_{11}$ assumed maximum values at points near the boundaries of the activated region. The maximum value of $T_{11}/\bar{c}_{11}^b$ equaled $1.9 \times 10^{-5}$; the maximum values of other stress components were nearly an order of magnitude lower than that of

$T_{11}$. Thus stresses induced in the top PZT are considerably below the yield stress of the material and its deformations are infinitesimal.

As is clear from the results presented in Table 1, the PZTs alter the natural frequencies of the structure; in some cases this may be advantageously used to shift the natural frequency of the structure away from the frequency of the external disturbance. Our analysis technique does not extend to the case when PZT patches that do not cover the entire plate surface are used.

## Conclusions

We have analyzed steady-state vibrations of a simply supported rectangular plate with PZT actuators bonded to its top and bottom surfaces. Three-dimensional equations of linear elasticity with mixed boundary conditions at the plate edges are solved by the method of Fourier series. It is assumed that PZTs can be modeled as thin layers and are perfectly bonded to the plate surfaces. The location and size of the optimum regions of the PZTs that should be excited with the minimum voltage to control the deflections of all points of the plate have been determined for four modes of vibration. For the voltage required to suppress the vibrations of all points to be minimum, the centroid of the excited PZT region should be located at points where the amplitude of initial vibrations of the simply supported plate is maximum. The method of Fourier series is difficult to apply to a plate with a clamped edge because of the difficulty in choosing expressions like those given by Eq. (11) for displacements that will satisfy boundary conditions identically.

## Acknowledgments

This work was supported by U.S. Army Research Office Grant DAAH04-93-G-0214 to the University of Missouri–Rolla and a matching grant from the Missouri Research and Training Center. Virginia Polytechnic Institute and State University acted as a subcontractor.

## References

[1]Baz, A., and Poh, S., "Performance of an Active Control System with Piezoelectric Actuators," *Journal of Sound and Vibration*, Vol. 126, No. 2, 1988, pp. 327–343.

[2]Tzou, H. S., and Tseng, C. I., "Distributed Modal Identification and Vibration Control of Continua: Piezoelectric Finite Element Formulation and Analysis," *Journal of Dynamic Systems, Measurement and Control*, Vol. 113, Sept. 1991, pp. 501–505.

[3]Crawley, E. F., and de Luis, J., "Use of Piezoelectric Actuators as Elements of Intelligent Structures," *AIAA Journal*, Vol. 25, No. 10, 1987, pp. 1373–1385.

[4]Srinivas, S., Rao, C. V. J., and Rao, A. K., "An Exact Analysis of Vibration of Simply-Supported Homogeneous and Laminated Thick Rectangular Plates," *Journal of Sound and Vibration*, Vol. 12, No. 2, 1970, pp. 257–269.

[5]Wittrick, W. H., "Analytical, Three-Dimensional Elasticity Solutions to Some Plate Problems, and Some Observations on Mindlin's Plate Theory," *International Journal of Solids and Structures*, Vol. 23, No. 4, 1987, pp. 441–464.

[6]Zhou, Y. S., and Tiersten, H. F., "Elastic Analysis of Laminated Composite Plates in Cylindrical Bending Due to Piezoelectric Actuators," *Smart Materials and Structures*, Vol. 3, No. 3, 1994, pp. 255–265.

[7]Yang, J. S., Batra, R. C., and Liang, X. Q., "The Cylindrical Bending Vibration of a Laminated Elastic Plate Due to Piezoelectric Actuators," *Smart Materials and Structures*, Vol. 3, No. 4, 1994, pp. 485–493.

[8]Yang, J. S., Batra, R. C., and Liang, X. Q., "The Vibration of a Simply Supported Rectangular Elastic Plate Due to Piezoelectric Actuators," *International Journal of Solids and Structures* (to be published).